



**STScI** | SPACE TELESCOPE  
SCIENCE INSTITUTE

Instrument Science Report COS 2024-13(v1)

# COS FUV Target Acquisition Monitoring: Cycles 25-31

---

Nick Indriolo<sup>1,2</sup>, S. Dieterich<sup>1</sup>, D. Sahnou<sup>1</sup>

<sup>1</sup>Space Telescope Science Institute, Baltimore, MD

<sup>2</sup>AURA for European Space Agency, STScI, USA

13 September 2024

---

## ABSTRACT

*Beginning in HST cycle 25, all COS FUV target acquisition algorithms work by stepping the target across the aperture, measuring the flux at each dwell point, calculating a flux-weighted centroid based on those measurements, and slewing the telescope to that centroid position. This entire procedure is performed by the flight software, and no images are recorded. To confirm that the target acquisition procedures are working as expected, each year we run a series of tests that simulate this process by acquiring exposures at specified offsets in the cross-dispersion direction. Here, we present the results of these tests from cycles 25, 26, 27, 28, 29, 30, and 31.*

---

## Contents

1. Introduction . . . . .	2
1.1 Summary of FUV TA Algorithms . . . . .	3
1.2 Description of FUV TA Yearly Monitor Programs . . . . .	5
1.3 Overview of the Cycle 25–31 FUV TA monitor programs . . . . .	6
2. Program Descriptions . . . . .	7
2.1 Cycle 25 . . . . .	7
2.2 Cycle 26 . . . . .	7
2.3 Cycle 27 . . . . .	8
2.4 Cycle 28 . . . . .	8
2.5 Cycle 29 . . . . .	9
2.6 Cycle 30 . . . . .	9
2.7 Cycle 31 . . . . .	10
3. Analysis & Results . . . . .	11
3.1 TA Subarray Confirmation . . . . .	11
3.2 Centering Accuracy: Simulated vs. Actual Acquisitions . . . . .	13
3.3 Centering Accuracy: Measurement by Cross-Correlation . . . . .	15
3.4 Cumulative Offset . . . . .	17
4. Summary . . . . .	17
Change History for COS ISR 2024-13 . . . . .	17
References . . . . .	19
Appendix A . . . . .	20

## 1. Introduction

The Cosmic Origins Spectrograph (COS) primary science aperture (PSA) has a diameter that corresponds to 2.5 arcsec on-sky. As the beam from an external source is not fully focused when passing through the aperture, deviations of  $> 0.4$  arcsec from aperture center will result in flux loss due to vignetting (see, e.g., Section 6.1 of the COS Instrument Handbook (IHB); Hirschauer et al., 2023). For targets with well-known coordinates (uncertainty  $\leq 0.4$  arcsec), the initial Hubble Space Telescope (HST) slew should place the target somewhere within the COS aperture. Once there, it is best practice to place the target at the center of the aperture. Centering the target in the along-dispersion (AD) direction ensures a robust wavelength solution is applied to spectral data, and centering in the cross-dispersion (XD) direction ensures a robust flux measurement. The centering requirement in the XD direction is  $\pm 0.3''$ , with a  $1\sigma$  goal of  $\pm 0.1''$ , while the requirements for the G130M, G160M, and G140L modes in the

AD direction are 0.106", 0.108", and 0.177", respectively. For a detailed description of the target centering requirements and their derivation, see either Penton & Keyes (2010) or Penton & Sahnou (2023).

The process of centering targets in the COS aperture is known as target acquisition (TA), and a variety of TA methods are available to users, as discussed in Section 8 of the COS IHB (Hirschauer et al., 2023). In this document, we focus on the pair of FUV TA modes that is used when target coordinates are known to within  $\leq 0.4$  arcsec. These are the ACQ/PEAKXD and ACQ/PEAKD procedures, which center the target in the XD and AD directions, respectively. They are always executed in this order, in succession, as a pair. Both methods work on dispersed light in the COS FUV channel, and both use a flux-weighted centroiding algorithm<sup>1</sup> to find the center of the aperture with respect to the initial target location.

### 1.1 Summary of FUV TA Algorithms

A brief description of the steps involved in these TA procedures is as follows. First, a 1-D pattern of exposures in the XD (or AD) direction is specified using the Astronomer's Proposal Tool (APT) Optional parameters NUM-POS and STEP-SIZE. The NUM-POS parameter defines the total number of dwell points (locations as which measurements are made), and the STEP-SIZE parameter defines the separation between those points in arcseconds. An ACCUM exposure is taken first at the zero offset position, and the number of counts is saved. The telescope then slews to the offset dwell points, and at each position an ACCUM exposure of the same length is taken and the number of counts is saved. Note that no exposures are saved as a part of this process; the only information returned is the number of counts at each dwell point and the location of each dwell point as offsets from the original center position in arcsec, which are saved in the first extension data array of the RAWACQ file associated with the acquisition sequence (see below for a description of how the number of counts at each dwell point is actually determined). Taking the number of counts at each dwell point,  $F_i$ , and the offset of that dwell point in arcsec,  $X_i$ , the flux-weighted centroid,  $C$ , is calculated as

$$C = \frac{\sum F_i X_i}{\sum F_i}. \quad (1)$$

The telescope then slews from the final dwell point by the amount necessary to place the location defined by  $C$  at the center of the aperture in the XD (or AD) axis. The difference between the final centered position and the original zero-offset position is saved in the primary extension header keywords ACQSLEWY and ACQSLEWX (slew offset in arcsec for the XD and AD directions, respectively) of the RAWACQ file. The actual slew amount from the final dwell point (given by  $C - X_{last}$ ) is also stored as ENDSLEWY and ENDSLEWX in the primary extension header.

---

<sup>1</sup>Prior to the start of operations at LP4 on 2017-10-02 at the beginning of cycle 25, the ACQ/PEAKXD procedure utilized a different centering method that was based on the separation between the PSA and WCA spectra, and is described in Keyes & Penton (2010).

**Table 1.** FUV Science Aperture Subarrays for LP5 and LP6.

LP	Segment	Grating	Cenwave	Subarray Name	XC	YC	XS	YS
5	FUVA	G130M	1291	A1	1201	471	4078	112
5	FUVA	G130M	1291	A2	8896	471	6555	112
5	FUVB	G130M	1291	B1	1501	530	5036	112
5	FUVB	G130M	1291	B2	7773	530	7060	112
6	FUVA	G160M	ALL	A1	1213	477	13799	112
6	FUVB	G160M	ALL	B1	1513	539	13332	112

Note. — Subarrays are defined in the raw detector coordinate system. The coordinates (XC, YC) specify the lower left corner of a subarray, while XS and YS give the size of the box in pixels in the X and Y directions, respectively. Values in this table were retrieved from the `spt` fits files associated with `rawacq` exposures, and are stored in the first extension header keywords `LQSUBnXC`, `LQSUBnYC`, `LQSUBnXS`, and `LQSUBnYS`, where  $n$  can be any integer from 0 to 7.

Proper calculation of the flux-weighted centroid requires that only flux from the target itself goes into the value  $F_i$ . For this reason, various regions on the detector must be excluded to prevent counts from sources other than the target (e.g., geocoronal Ly- $\alpha$ , hot spots, stim pulses) from contributing to the calculation. This is done by defining subarrays<sup>2</sup>, such that only counts falling inside these regions are included in the centroiding calculation. The subarrays used at lifetime positions (LPs) 5 and 6 are presented in Table 1, while those for LP1–4 can be found in Penton & Sahnou (2023). Note that the subarrays are defined in raw detector coordinates, not the user coordinates provided in the `RAWX` and `RAWY` columns of `COS TIME-TAG` data arrays. No correction of any type (e.g., thermal, geometric, walk) is applied to the data during this analysis. The transformation between detector and user coordinates for the FUV detector is given by  $X_{user} = 16383 - X_{detector}$  and  $Y_{user} = Y_{detector}$ .

Finally, the value  $F_i$  used in equation 1 can be modified if a different centroiding algorithm is selected in `APT` by the user. The `CENTER=FLUX-WT` algorithm works exactly as described above, while the `CENTER=FLUX-WT-FLR` algorithm takes the minimum value of  $F$  from all dwell points and subtracts that value from every  $F_i$  (including the minimum itself). Mathematically speaking,  $F_i$  becomes  $F_i - \min(F)$ , and it is these floor-subtracted values that are stored in the first extension data array of the `RAWACQ` file, while  $\min(F)$  can be found in the primary extension header keyword `ACQFLOOR`.

<sup>2</sup>maximum of 4 per each detector segment, but only 1 or 2 currently in use

## *1.2 Description of FUV TA Yearly Monitor Programs*

The purpose of the annual FUV TA monitor program is to test that the procedures described above are working as expected. The general method for TA testing works as follows. First, the target is centered in both the XD and AD directions using the NUV imaging mode TA (ACQ/IMAGE). Then, an FUV exposure is taken with the spectrum at the centered position to serve as the reference. The telescope is offset in the cross dispersion direction by an angle that matches one of the standard ACQ/PEAKXD patterns and another exposure is taken. This is repeated for all of the dwell points in the specific ACQ/PEAKXD pattern that is being tested. Throughout this document, we will refer to the above sequence of exposures as a simulated acquisition sequence. After completing the simulated acquisition sequence, an actual ACQ/PEAKXD sequence using the same dwell pattern is executed. Finally, another exposure is taken with the spectrum at the position considered to be centered by the acquisition procedure<sup>3</sup>. This pairing of simulated and actual acquisition sequences is repeated for every combination of LP and grating that can be used for FUV TA during the current observing cycle. For some LP+grating combinations, different sets of ACQ/PEAKXD patterns are tested. Note that in cycles 25–31 there were no simulated ACQ/PEAKXD sequences.

Using these data, we perform four checks on the TA procedure. The first check is to ensure that at all dwell points the full flux in the cross-dispersion profile of the external target falls within the subarrays used for centering that mode. This is done by simple image inspection, as illustrated in Figures 1–3. Note that this inspection also includes checking to ensure that all flux from sources other than the target (e.g., geocoronal Ly- $\alpha$  emission, hot spots) is excluded from the subarrays.

The second check is for the accuracy of the target centering. Using the exposures taken to simulate an ACQ/PEAKXD sequence, the number of counts at each dwell point is measured as described above<sup>4</sup>, and the resulting values are used to calculate the flux-weighted centroid via equation 1. The calculated centroid is compared to the ACQSLEWY value returned by the actual ACQ/PEAKXD sequence that executes right after the simulated sequence. The simulated and actual sequences are doing the same thing, and so should find the same centroid position.

The third check is for centering of the spectrum immediately following any of the ACQ sequences in the visit (i.e., how well does the acquisition work). The centered exposure observed right after the initial NUV ACQ/IMAGE is taken to be the reference, and all “centered” spectra taken after subsequent ACQ sequences are cross-correlated to that initial spectrum (see Dieterich, et al. 2024 for details). Ideally this check would be done in both the AD and XD directions, but due to complications discussed in Section 3.3 only the XD test is presented here.

The fourth check is that the FUV ACQ sequences are centering the target to within

---

<sup>3</sup>In some cases the centered exposure taken after the actual acquisition sequence is also part of another simulated acquisition sequence.

<sup>4</sup>Note that all exposures must be truncated to have the same exposure length.

requirements, assuming that the center position found by the initial NUV ACQ/IMAGE procedure is correct. For all subsequent FUV and NUV acquisition sequences during a visit, the cumulative movement imparted by each ACQ is tracked, and compared to the 0.3" requirement and 0.1" goal in the XD direction, and the grating-specific requirements in the AD direction.

### ***1.3 Overview of the Cycle 25–31 FUV TA monitor programs***

The cycle 25 FUV TA monitor was executed as program 15386, during which ACQ/PEAKXD at LP4 (G130M/1291, G160M/1600, & G140L/1280) was tested. A full description of the cycle 25 testing sequence is provided in Table A1.

The cycle 26 FUV TA monitor was executed as program 15537, during which ACQ/PEAKXD at LP4 (G130M/1291, G160M/1600, & G140L/1280) was tested. A full description of the cycle 26 testing sequence is provided in Table A2.

The cycle 27 FUV TA monitor was executed as program 15775, during which ACQ/PEAKXD at LP4 (G130M/1291, G160M/1600, & G140L/1280) was tested. A full description of the cycle 27 testing sequence is provided in Table A3.

The cycle 28 FUV TA monitor was executed as program 16326, during which ACQ/PEAKXD at LP4 (G130M/1291, G160M/1600, & G140L/1280) was tested. A full description of the cycle 28 testing sequence is provided in Table A4.

The cycle 29 FUV TA monitor was executed as program 16831, during which ACQ/PEAKXD at LP4 (G160M/1600 & G140L/1280) and LP5 (G130M/1291) were tested. A full description of the cycle 29 testing sequence is provided in Table A5. While the default location for G140L science spectra moved to LP3 on 2024-10-04 at the beginning of cycle 29, target acquisition with G140L remains at LP4 (this is to account for the different ACQ/PEAKXD procedures in use at LP1-3 (Keyes & Penton 2010) and at LP4-6). Due to an omission in the program definition within APT, the manual dwell point exposures for G140L were taken at LP3 instead of LP4. As a result, they do not test the actual ACQ/PEAKXD procedure in use, and so are not further analyzed.

The cycle 30 FUV TA monitor was executed as program 16942, during which ACQ/PEAKXD at LP4 (G160M/1600 & G140L/1280) and LP5 (G130M/1291) were tested. A full description of the cycle 30 testing sequence is provided in Table A6.

The cycle 31 FUV TA monitor was executed as program 17582, during which ACQ/PEAKXD at LP4 (G160M/1600 & G140L/1280), LP5 (G130M/1291), and LP6 (G160M/1600) were tested. A full description of the cycle 31 testing sequence is provided in Table A7.

## 2. Program Descriptions

### 2.1 Cycle 25

Observations from program 15386 were executed in December 2017 and February 2018. This program originally consisted of the single two-orbit visit 25. Due to a partial failure (second orbit), the unperformed tests were rescheduled as visit 90, which completely failed, but were successfully executed in the single-orbit visit 91. The successful portion of visit 25 tests the TA procedures at LP4 for G130M, while visit 91 tests the procedures at LP4 for G140L and G160M.

Visit 25 begins with an NUV ACQ/IMAGE to center the target and then a confirmation NUV image that includes the PtNe lamp. Switching to the FUV detector and using the G130M/1291 setting, simulated and actual ACQ/PEAKXD sequences with NUM-POS=3 and STEP-SIZE=1.3'' are performed in succession. These are followed by simulated and actual ACQ/PEAKXD sequences with NUM-POS=5 and STEP-SIZE=0.9'', after which a centered exposure is taken. The successful portion of the visit concludes with an actual ACQ/PEAKD sequence with NUM-POS=5 and STEP-SIZE=0.9'', and a final centered exposure.

The first half of visit 91 begins with an NUV ACQ/IMAGE to center the target and a confirmation NUV image. Switching to the FUV detector and using the G140L/1280 setting, simulated and actual ACQ/PEAKXD sequences with NUM-POS=3 and STEP-SIZE=1.3'' are performed in succession, after which a centered exposure is taken. The second half of visit 91 performs the exact same sequence of exposures as the first half, but using the G160M/1600 setting instead. Table A1 provides more details regarding the full series of exposures taken in program 15386.

### 2.2 Cycle 26

Observations from program 15537 were executed in early January 2019. This program consisted of the single two-orbit visit 25. It tests the TA procedures at LP4 for G130M, G140L, and G160M modes.

The first orbit of visit 25 begins with an NUV ACQ/IMAGE to center the target and then a confirmation NUV image that includes the PtNe lamp. Switching to the FUV detector and using the G130M/1291 setting, simulated and actual ACQ/PEAKXD sequences with NUM-POS=3 and STEP-SIZE=1.3'' are performed in succession. These are followed by simulated and actual ACQ/PEAKXD sequences with NUM-POS=5 and STEP-SIZE=0.9'', after which a centered exposure is taken. The first orbit concludes with an actual ACQ/PEAKD sequence with NUM-POS=5 and STEP-SIZE=0.9'', and a final centered exposure.

The second orbit of visit 25 begins with an NUV ACQ/IMAGE to center the target and a confirmation NUV image. Switching to the FUV detector and using the G140L/1280 setting, simulated and actual ACQ/PEAKXD sequences with NUM-POS=3

and STEP-SIZE=1.3'' are performed in succession, after which a centered exposure is taken. This exact same sequence, including the NUV ACQ/IMAGE, is then repeated using the G160M/1600 setting. Table A2 provides more details regarding the full series of exposures taken in program 15537.

### **2.3 Cycle 27**

Observations from program 15775 were executed in mid January 2020. This program consisted of the single two-orbit visit 25. It tests the TA procedures at LP4 for G130M, G140L, and G160M modes.

The first orbit of visit 25 begins with an NUV ACQ/IMAGE to center the target and then a confirmation NUV image that includes the PtNe lamp. Switching to the FUV detector and using the G130M/1291 setting, simulated and actual ACQ/PEAKXD sequences with NUM-POS=3 and STEP-SIZE=1.3'' are performed in succession. These are followed by simulated and actual ACQ/PEAKXD sequences with NUM-POS=5 and STEP-SIZE=0.9'', after which a centered exposure is taken. The first orbit concludes with an actual ACQ/PEAKD sequence with NUM-POS=5 and STEP-SIZE=0.9'', and a final centered exposure.

The second orbit of visit 25 begins with an NUV ACQ/IMAGE to center the target and a confirmation NUV image. Switching to the FUV detector and using the G140L/1280 setting, simulated and actual ACQ/PEAKXD sequences with NUM-POS=3 and STEP-SIZE=1.3'' are performed in succession, after which a centered exposure is taken. This exact same sequence, including the NUV ACQ/IMAGE, is then repeated using the G160M/1600 setting. Table A3 provides more details regarding the full series of exposures taken in program 15775.

### **2.4 Cycle 28**

Observations from program 16326 were executed in early January 2021. This program consisted of the single two-orbit visit 25. It tests the TA procedures at LP4 for G130M, G140L, and G160M modes.

The first orbit of visit 25 begins with an NUV ACQ/IMAGE to center the target and then a confirmation NUV image that includes the PtNe lamp. Switching to the FUV detector and using the G130M/1291 setting, simulated and actual ACQ/PEAKXD sequences with NUM-POS=3 and STEP-SIZE=1.3'' are performed in succession. These are followed by simulated and actual ACQ/PEAKXD sequences with NUM-POS=5 and STEP-SIZE=0.9'', after which a centered exposure is taken. The first orbit concludes with an actual ACQ/PEAKD sequence with NUM-POS=5 and STEP-SIZE=0.9'', and a final centered exposure.

The second orbit of visit 25 begins with an NUV ACQ/IMAGE to center the target and a confirmation NUV image. Switching to the FUV detector and using the

G140L/1280 setting, simulated and actual ACQ/PEAKXD sequences with NUM-POS=3 and STEP-SIZE=1.3'' are performed in succession, after which a centered exposure is taken. This exact same sequence, including the NUV ACQ/IMAGE, is then repeated using the G160M/1600 setting. Table A4 provides more details regarding the full series of exposures taken in program 16326.

### ***2.5 Cycle 29***

Observations from program 16831 were executed in early January of 2022. This program consists of two visits. Visit 01 tests TA procedures at LP5 for G130M, while visit 02 tests procedures at LP4 for G160M, and was also intended to test procedures at LP4 for G140L. Visit 01 begins with an NUV ACQ/IMAGE to center the target and then a confirmation NUV image that includes the PtNe lamp. Switching to the FUV detector and using the G130M/1291 setting, simulated and actual ACQ/PEAKXD sequences with NUM-POS=3 and STEP-SIZE=1.3'' are performed in succession. These are followed by simulated and actual ACQ/PEAKXD sequences with NUM-POS=5 and STEP-SIZE=0.9'', after which a centered exposure is taken. The visit concludes with an actual ACQ/PEAKD sequence with NUM-POS=5 and STEP-SIZE=0.9'', and a final centered exposure.

The first half of visit 02 was intended to test some ACQ/PEAKXD sequences at LP4 using G140L/1280. However, the default location for G140L science exposures was moved to LP3 starting in this cycle, while the G140L TA location remained at LP4. Because the LP was not specified in APT (i.e., left as the default), all of the simulated acquisition exposures were taken at LP3, while the actual acquisition sequences executed at LP4. Because of different gain properties of the detector in the two regions, the simulated and actual acquisition sequences are not measuring the same centroid, and so they cannot be used to test the accuracy of the acquisition procedure here. We do not consider these data further in this report.

The second half of visit 02 begins with an NUV ACQ/IMAGE to center the target and a confirmation NUV image. Switching to the FUV detector and using the G160M/1600 setting at LP4, simulated and actual ACQ/PEAKXD sequences with NUM-POS=3 and STEP-SIZE=1.3'' are performed in succession, after which a centered exposure is taken. The visit concludes with an actual ACQ/PEAKD sequence with NUM-POS=5 and STEP-SIZE=0.9'', and a final centered exposure. Table A5 provides more details regarding the full series of exposures taken in program 16831.

### ***2.6 Cycle 30***

Observations from program 16942 were executed in January 2023. This program consisted of three visits. Visit 01 tests the TA procedures at LP5 for the G130M mode. Visit 02 tests the TA procedures at LP4 for the G140L and G160M modes. Visit 03 is a repeat of program 16851 visit 02 (*COS LP6 FUV Target Acquisition Enabling and*

*Verification*), and will be presented in a separate report.

Visit 01 begins with an NUV ACQ/IMAGE to center the target and then a confirmation NUV image that includes the PtNe lamp. Switching to the FUV detector and using the G130M/1291 setting, simulated and actual ACQ/PEAKXD sequences with NUM-POS=3 and STEP-SIZE=1.3'' are performed in succession. These are followed by simulated and actual ACQ/PEAKXD sequences with NUM-POS=5 and STEP-SIZE=0.9'', after which a centered exposure is taken. The visit concludes with an actual ACQ/PEAKD sequence with NUM-POS=5 and STEP-SIZE=0.9'', and a final centered exposure.

The first orbit of visit 02 begins with an NUV ACQ/IMAGE to center the target and a confirmation NUV image. Switching to the FUV detector and using the G140L/1280 setting, a centered spectrum is taken at the LP3 position (default for G140L science exposures). Moving back to LP4, simulated and actual ACQ/PEAKXD sequences with NUM-POS=3 and STEP-SIZE=1.3'' are performed in succession, after which a centered exposure at LP3 is taken. Again at LP4, simulated and actual ACQ/PEAKXD sequences with NUM-POS=5 and STEP-SIZE=0.9'', after which a final centered exposure at LP3 is taken.

The second orbit of visit 02 again begins with an NUV ACQ/IMAGE to center the target and a confirmation NUV image. Switching to the FUV detector and using the G160M/1600 setting at LP4, simulated and actual ACQ/PEAKXD sequences with NUM-POS=3 and STEP-SIZE=1.3'' are performed in succession, after which a centered exposure is taken. The visit concludes with an actual ACQ/PEAKD sequence with NUM-POS=5 and STEP-SIZE=0.9'', and a final centered exposure. Table A6 provides more details regarding the full series of exposures taken in program 16942.

## ***2.7 Cycle 31***

Observations from program 17582 were executed in January 2024. This program consisted of three visits. Visit 01 tests the TA procedures at LP5 for the G130M mode. Visit 02 tests the TA procedures at LP4 for the G160M mode. The two-orbit visit 03 tests the TA procedures at LP4 for the G140L mode and at LP6 for the G160M mode.

Visit 01 begins with an NUV ACQ/IMAGE to center the target and then a confirmation NUV image that includes the PtNe lamp. Switching to the FUV detector and using the G130M/1291 setting at LP5, simulated and actual ACQ/PEAKXD sequences with NUM-POS=3 and STEP-SIZE=1.3'' are performed in succession. These are followed by simulated and actual ACQ/PEAKXD sequences with NUM-POS=5 and STEP-SIZE=0.9'', after which a centered exposure is taken. The visit concludes with an actual ACQ/PEAKD sequence with NUM-POS=5 and STEP-SIZE=0.9'', and a final centered exposure.

Visit 02 begins with an NUV ACQ/IMAGE to center the target and a confirmation NUV image. Switching to the FUV detector and using the G160M/1600 setting at LP4, simulated and actual ACQ/PEAKXD sequences with NUM-POS=3 and STEP-

SIZE=1.3'' are performed in succession, after which a centered exposure is taken. The visit concludes with an actual ACQ/PEAKD sequence with NUM-POS=5 and STEP-SIZE=0.9'', and a final centered exposure.

The first orbit of visit 03 begins with an NUV ACQ/IMAGE to center the target and a confirmation NUV image. Switching to the FUV detector and using the G140L/1280 setting at LP4, simulated and actual ACQ/PEAKXD sequences with NUM-POS=3 and STEP-SIZE=1.3'' are performed in succession. These are followed by simulated and actual ACQ/PEAKXD sequences with NUM-POS=5 and STEP-SIZE=0.9'', after which a centered exposure is taken.

The second orbit of visit 03 again begins with an NUV ACQ/IMAGE to center the target and a confirmation NUV image. Switching to the FUV detector and using the G160M/1600 setting at LP6, simulated and actual ACQ/PEAKXD sequences with NUM-POS=3 and STEP-SIZE=1.3'' are performed in succession, after which a centered exposure is taken. The visit concludes with an actual ACQ/PEAKD sequence with NUM-POS=5 and STEP-SIZE=0.9'', and a final centered exposure. Table A7 provides more details regarding the full series of exposures taken in program 17582.

### **3. Analysis & Results**

Here we present the four checks mentioned in the Introduction.

#### ***3.1 TA Subarray Confirmation***

The first check is a visual inspection of the FUV images to ensure that the TA subarrays are defined appropriately. Figures 1, 2, and 3 demonstrate how this is done for three example cases. Images like these are generated for every FUV exposure in each TA program and are checked to (1) confirm that target flux is within the TA subarrays in the XD direction for all offset positions, and (2) confirm that flux from sources other than the target is excluded from the subarrays. All FUV exposures pass these checks.

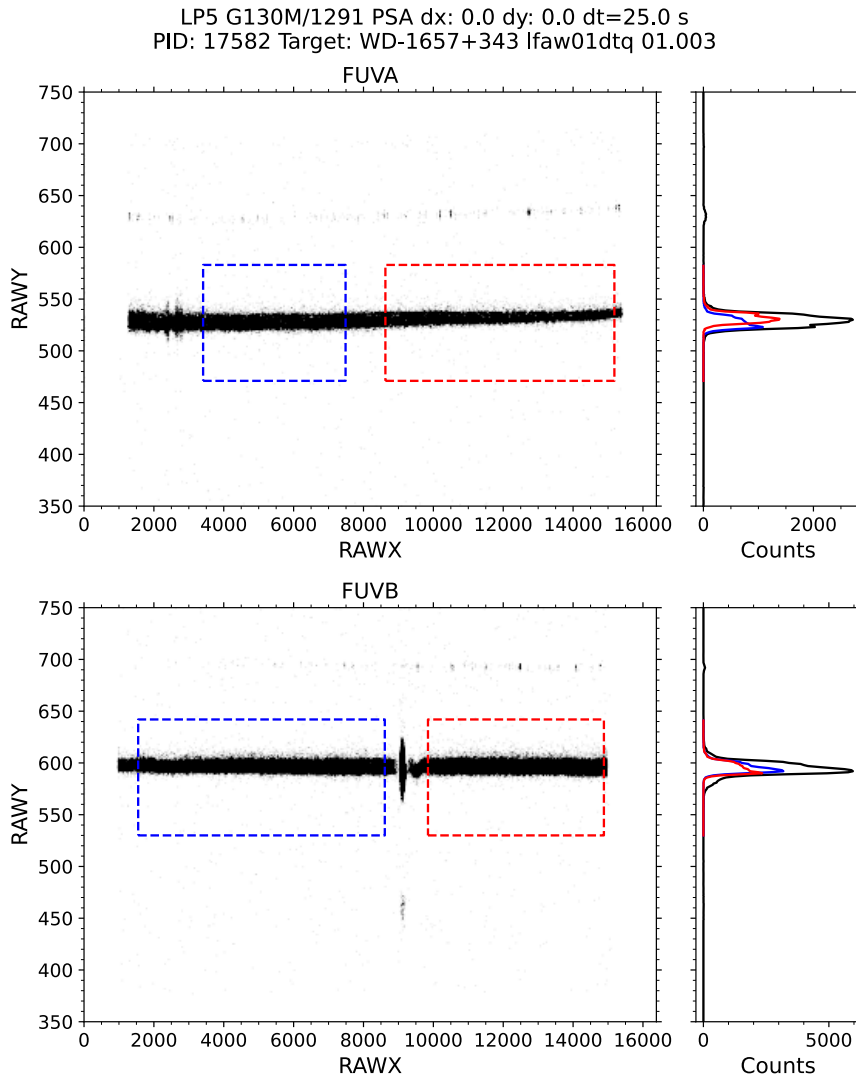


**Figure 1.** Example 2D spectral images from the cycle 31 FUV TA program. The FUVB segment is on top, and the FUVB segment on bottom. The subarrays (converted to user coordinates here) are shown as blue and red dashed boxes. In the right hand panels, the black curve shows the cross-dispersion profile from the entire image, while the red and blue curves show the profiles within the respective boxes. A PtNe lamp emission line spectrum from the wavelength calibration aperture (WCA) can be seen above the target spectrum on both segments. The bright spots near  $RAWX \sim 2500$  on FUVB are due to geocoronal O I emission. Geocoronal Ly- $\alpha$  emission passing through the PSA and BOA (bright object aperture) causes the spots at  $(RAWX, RAWY) \approx (9000, 600)$  and  $(9000, 460)$ , respectively.

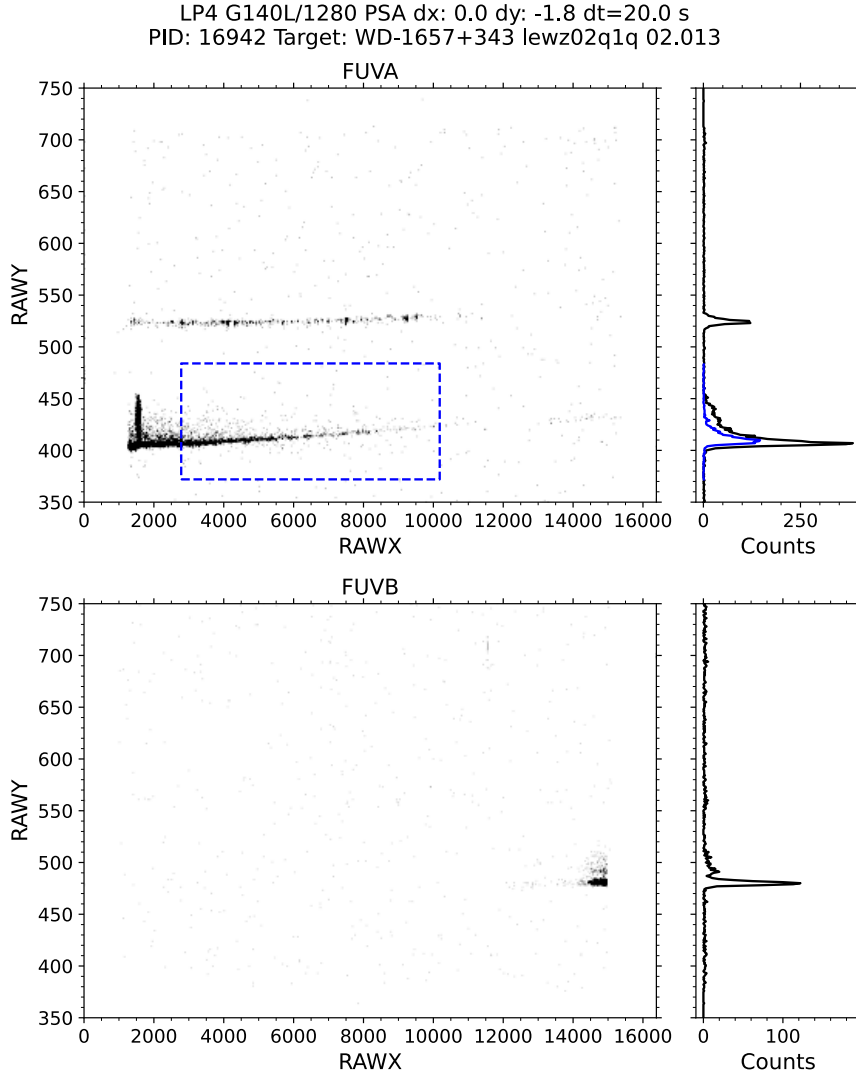


**Figure 2.** Same as Figure 1, but showing a G140L/1280 spectrum offset by  $-1.8''$  in the XD direction. There are no subarrays on FUVB for G140L modes. In the top panel the spectrum appears at the very bottom of the aperture (the extent of which is traced by the geocoronal Ly- $\alpha$  line at  $RAWX \approx 1500$ ), as expected given the offset.

### 3.2 Centering Accuracy: Simulated vs. Actual Acquisitions

The second check is a comparison between the flux-weighted centroids determined by simulated and actual acquisition sequences executed in succession. Results from every TA sequence simulated in cycles 25–31 are presented in Table 2. The slew performed by the telescope following an actual acquisition is given in the ACQ centroid column. This value is compared to the entries in two Test Centroid columns. Both columns

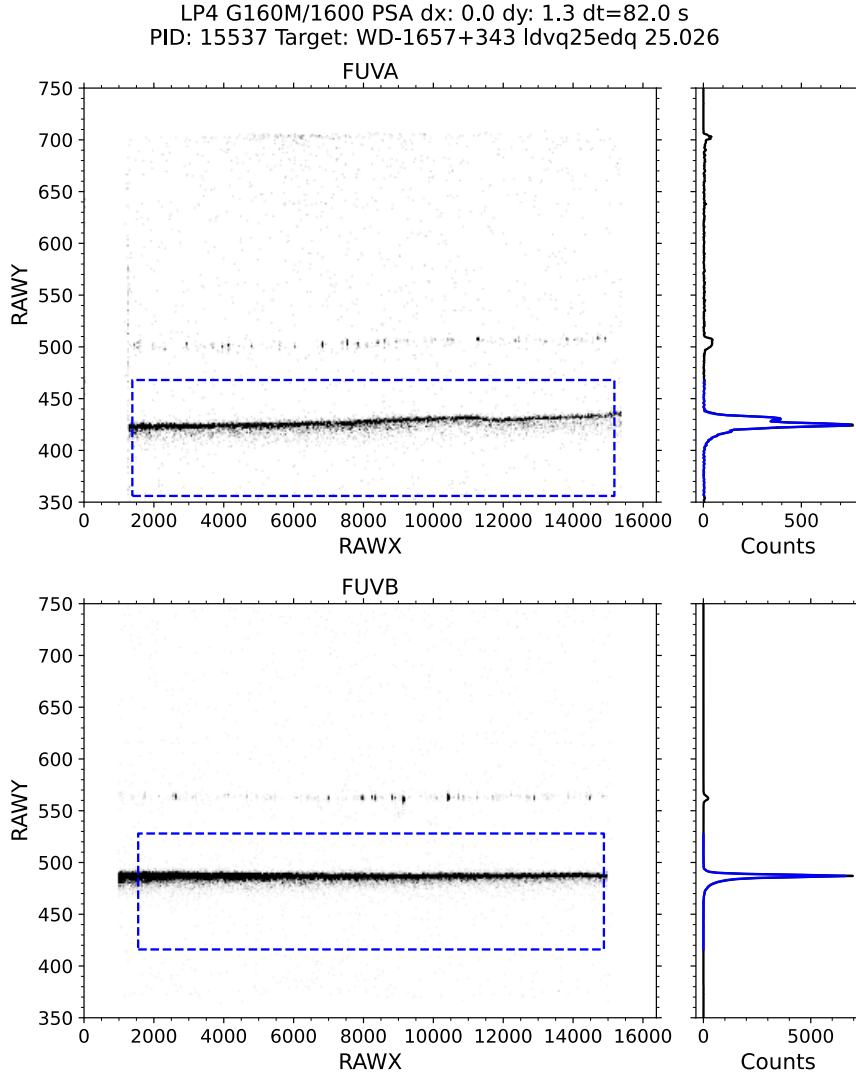


**Figure 3.** Same as Figure 1, but showing a G160M/1600 spectrum offset by 1.3'' in the XD direction.

present results calculated using data from the simulated acquisition sequence exposures and equation 1, one each for the two different centroiding algorithms previously described. The Centroid algorithm column lists which algorithm was used during the actual acquisition (primary header CENTER keyword), to facilitate direct comparison between the simulated and actual results. Estimates of the Poisson uncertainty in the flux-weighted centroids are calculated using the equation given in Proffitt et al. (2015), modified to account for the lack of a background subtraction in our analysis, and are also given in the Test Centroid columns. Note that the ACQSLEWY values presented here in the ACQ Centroid column give the distance that the *telescope* is slewed to place the target at the center of the aperture. The POSTARG2 values from the simulated

acquisition sequences that go into calculating the flux-weighted centroid give the offset of the *target* with respect to aperture center, and so have the opposite sign convention. The Test Centroid columns have been multiplied by  $-1$  following the use of equation 1 so that the results are directly comparable. For every simulated TA sequence, the centroid computed using the same algorithm as the actual TA sequences and the centroid found by the actual TA sequence agree to within  $0.024''$ .

### ***3.3 Centering Accuracy: Measurement by Cross-Correlation***

The third check is a comparison between the reference spectrum (taken following the initial NUV ACQ/IMAGE, and all “centered” spectra taken right after subsequent ACQ sequences. In all cases, the spectra should be located at the same position on the detector. This test is done by collapsing the data within the subarrays along the dispersion direction to create cross-dispersion profiles on the FUV A and FUV B segments for each exposure. The cross-dispersion profile from the test exposure is cross correlated with the cross-dispersion profile from the reference exposure, and a gaussian fit is performed to the resulting cross-correlation function to determine the offset in the XD direction between both exposures. This analysis is done separately for the FUV A and FUV B segments, and the mean offset of both is reported in Table 3. While the cross-correlation offset is measured in pixels, the offset in arcsec is computed using the detector plate scales from the COS IHB (Hirschauer et al. 2023). The maximum deviation between reference and test spectra in the XD direction during cycles 25–31 was  $0.201''$ , within the  $0.3''$  requirement. As a result, we conclude that the FUV TA procedures are successfully centering targets in the XD direction.

Ideally, a 2D cross-correlation would be performed to measure the offset between spectra in both the XD and AD directions. However, there are multiple factors that make performing cross-correlation in the AD direction untenable. First, the target used in these programs, WD 1657+343, has a spectrum that is featureless in the UV aside from broad hydrogen absorption lines (Bohlin et al. 2020), meaning there are no narrow wavelength-specific features to cross-correlate. This issue is exacerbated by the fixed pattern noise on the COS detector (e.g., grid-wire shadows and fiber bundle hex patterns; Hirschauer et al. 2023), which could bias the cross-correlation to features of the detector itself, rather than features of the spectrum. Lastly, the optics select mechanism 1 (OSM1) is known to slowly rotate during exposures, causing the spectrum to drift in the AD direction. The magnitude of this OSM1 drift can be anywhere from 0 to 6 pixels over the course of  $\sim 3000$  s exposures (Rowlands et al. 2024). While the individual exposures in these programs are much shorter, OSM1 drift will still occur over the course of all exposures taken at the same CENWAVE setting during a visit. This can potentially be accounted for by using the shift values measured by CalCOS (SHIFT1A and SHIFT1B keywords in the first extension header of `x1d` files), but it adds further complexity to the analysis. Also, this cannot be done for observations made at LP6, as concurrent WCA spectra are not obtained there. Given these complications,

**Table 2.** FUV ACQ/PEAKXD Testing Results

LINENUM	LP	Grating	NUMPOS/ STEP SIZE	Centroid algorithm	ACQ Centroid (arcsec)	Test Centroid FLX-WT (arcsec)	Test Centroid FLX-WT-FLR (arcsec)	Integration Time (s)
Cycle 25 Program 15386								
25.006	4	G130M	3/1.3	FLUXWT	0.091	0.077±0.002	0.155±0.002	25
25.012	4	G130M	5/0.9	FLUXFLR	-0.041	-0.041±0.002	-0.047±0.002	25
91.006	4	G140L	3/1.3	FLUXWT	0.051	0.055±0.005	0.115±0.003	20
91.013	4	G160M	3/1.3	FLUXWT	0.09	0.082±0.002	0.164±0.001	82
Cycle 26 Program 15537								
25.006	4	G130M	3/1.3	FLUXWT	0.071	0.073±0.002	0.147±0.002	25
25.012	4	G130M	5/0.9	FLUXFLR	-0.034	-0.018±0.002	-0.021±0.002	25
25.021	4	G140L	3/1.3	FLUXWT	0.076	0.084±0.005	0.165±0.003	20
25.028	4	G160M	3/1.3	FLUXWT	0.117	0.093±0.002	0.184±0.001	82
Cycle 27 Program 15775								
25.006	4	G130M	3/1.3	FLUXWT	0.099	0.090±0.002	0.177±0.002	25
25.012	4	G130M	5/0.9	FLUXFLR	-0.044	-0.034±0.002	-0.039±0.002	25
25.021	4	G140L	3/1.3	FLUXWT	0.096	0.102±0.005	0.194±0.004	20
25.028	4	G160M	3/1.3	FLUXWT	0.062	0.062±0.002	0.131±0.001	82
Cycle 28 Program 16326								
25.006	4	G130M	3/1.3	FLUXWT	0.048	0.057±0.002	0.119±0.001	25
25.012	4	G130M	5/0.9	FLUXFLR	-0.025	-0.014±0.002	-0.016±0.002	25
25.021	4	G140L	3/1.3	FLUXWT	0.085	0.062±0.005	0.126±0.003	20
25.028	4	G160M	3/1.3	FLUXWT	0.081	0.073±0.002	0.150±0.001	82
Cycle 29 Program 16831								
01.006	5	G130M	3/1.3	FLUXWT	0.159	0.156±0.002	0.274±0.002	25
01.012	5	G130M	5/0.9	FLUXFLR	-0.059	-0.048±0.002	-0.055±0.002	25
02.019	4	G160M	3/1.3	FLUXWT	0.036	0.041±0.002	0.089±0.001	82
Cycle 30 Program 16942								
01.006	5	G130M	3/1.3	FLUXWT	0.011	0.007±0.002	0.016±0.001	25
01.012	5	G130M	5/0.9	FLUXFLR	-0.012	-0.004±0.002	-0.004±0.002	25
02.007	4	G140L	3/1.3	FLUXWT	-0.109	-0.126±0.005	-0.231±0.004	20
02.014	4	G140L	5/0.9	FLUXFLR	0.034	0.030±0.004	0.035±0.004	20
02.021	4	G160M	3/1.3	FLUXWT	0.04	0.043±0.002	0.094±0.001	82
Cycle 31 Program 17582								
01.006	5	G130M	3/1.3	FLUXWT	0.013	0.001±0.002	0.002±0.000	25
01.012	5	G130M	5/0.9	FLUXFLR	0.003	-0.008±0.002	-0.010±0.002	25
02.006	4	G160M	3/1.3	FLUXWT	-0.03	-0.036±0.002	-0.079±0.001	82
03.006	4	G140L	3/1.3	FLUXWT	-0.03	-0.013±0.005	-0.029±0.002	20
03.012	4	G140L	5/0.9	FLUXFLR	0.01	0.015±0.004	0.018±0.004	20
03.019	6	G160M	3/1.3	FLUXWT	0.095	0.093±0.002	0.180±0.001	82

Note. — The LINENUM column refers to the actual ACQ exposure, and the ACQ Centroid column is the result from that acquisition stored in the primary header ACQSLEWY keyword. The Test Centroid columns are the results from calculations done using the simulated ACQ sequences. Note that ACQSLEWY gives the offset of the telescope in arcsec, while POSTARG2 (XD offset in Tables A1–A7) is the offset of the target in arcsec. After using equation 1, the result must be multiplied by  $-1$  for direct comparison to ACQSLEWY. This conversion has already been applied to the Test Centroid columns. The maximum difference between centroids calculated from the actual and simulated TA sequences when considering the same algorithm is 0.024”.

we do not attempt to confirm centering in the AD direction via cross-correlation.

### ***3.4 Cumulative Offset***

The fourth and final check is that all ACQ sequences executed during a visit place the target at the “same” location within the aperture. Here, we consider the initial position identified by the first NUV ACQ/IMAGE sequence to be the reference position at  $(AD, XD) = (0, 0)$ . Each subsequent ACQ applies an offset with respect to the “centered” position identified by the previous ACQ, such that there is a cumulative displacement from the original center over the course of a visit. We check that all cumulative offsets throughout a visit remain within the AD and XD requirements specified in the Introduction. Figure 4 shows that for all successful visits executed as part of the FUV TA monitor program over the past seven cycles the cumulative offsets remain within requirements, and only in a few cases do they not meet the  $1\sigma$  XD centering goal. As a result, we conclude that the NUV and FUV TA sequences are centering the target to the same location to within requirements.

## **4. Summary**

We have analyzed the data from the FUV TA monitoring program in cycles 25 through 31, performing four checks to determine whether or not FUV TA sequences are operating as expected.

1. All TA subarrays in use at LP4, LP5, and LP6 are defined properly to capture the cross-dispersion profile of the external target at all XD offset positions, and to exclude flux from sources other than the external target.
2. Flux-weighted centroids calculated from simulated TA sequences are in agreement with centroids found by actual TA sequences to within  $0.025''$ , so the algorithms are performing as expected.
3. Offsets in the XD direction measured between “centered” spectra are all within the  $0.3''$  requirement, with a maximum separation of  $0.201''$
4. The cumulative offset caused by every Acquisition sequence that is executed during a visit is within the AD and XD requirements, such that they are placing the target at the “same” location within the aperture.

Our tests indicate that the FUV TA procedures are working well.

## **Change History for COS ISR 2024-13**

Version 1: 13 September 2024- Original Document

**Table 3.** Offsets Measured between Centered Spectra

Grating	LP	Reference Exposure	Test Exposure	XD Offset (arcsec)
Cycle 25 Program 15386				
G130M	4	ldqq25gdq	ldqq25glq	0.127
G130M	4	ldqq25gdq	ldqq25h3q	0.061
G130M	4	ldqq25gdq	ldqq25h8q	0.045
G140L	4	ldqq91vpq	ldqq91vyq	0.072
G160M	4	ldqq91w4q	ldqq91wcq	0.135
Cycle 26 Program 15537				
G130M	4	ldvq25cyq	ldvq25d6q	0.102
G130M	4	ldvq25cyq	ldvq25dmq	0.035
G130M	4	ldvq25cyq	ldvq25dqq	0.024
G140L	4	ldvq25dxq	ldvq25e5q	0.124
G160M	4	ldvq25ebq	ldvq25f6q	0.138
Cycle 27 Program 15775				
G130M	4	le5e25k9q	le5e25khq	0.134
G130M	4	le5e25k9q	le5e25ktq	0.058
G130M	4	le5e25k9q	le5e25kxq	0.042
G140L	4	le5e25l3q	le5e25l1bq	0.157
G160M	4	le5e25l1hq	le5e25l1pq	0.085
Cycle 28 Program 16326				
G130M	4	lef925weq	lef925wmq	0.075
G130M	4	lef925weq	lef925wyq	0.036
G130M	4	lef925weq	lef925x2q	0.024
G140L	4	lef925x8q	lef925xgq	0.138
G160M	4	lef925xm1q	lef925xuq	0.118
Cycle 29 Program 16831				
G130M	5	ler201apq	ler201axq	0.201
G130M	5	ler201apq	ler201b9q	0.140
G130M	5	ler201apq	ler201c0q	0.138
G140L	3	ler202naq	ler202niq	0.089
G140L	3	ler202naq	ler202nuq	0.042
G160M	4	ler202o0q	ler202o8q	0.081
G160M	4	ler202o0q	ler202ocq	0.085
Cycle 30 Program 16942				
G130M	5	lewz01i8q	lewz01igq	0.027
G130M	5	lewz01i8q	lewz01isq	-0.010
G130M	5	lewz01i8q	lewz01izq	-0.021
G140L	4	lewz02pj1q	lewz02ptq	-0.122
G160M	4	lewz02qbq	lewz02qkq	0.083
G160M	4	lewz02qbq	lewz02rbq	0.079
Cycle 31 Program 17582				
G130M	5	lfaw01dtq	lfaw01e1q	0.012
G130M	5	lfaw01dtq	lfaw01edq	-0.032
G130M	5	lfaw01dtq	lfaw01ehq	-0.048
G160M	4	lfaw02aeq	lfaw02apq	-0.019
G160M	4	lfaw02aeq	lfaw02atq	-0.026
G140L	4	lfaw03fiq	lfaw03fqq	-0.025
G140L	4	lfaw03fiq	lfaw03g3q	-0.038
G160M	6	lfaw03ggq	lfaw03goq	0.122
G160M	6	lfaw03ggq	lfaw03gsq	0.112

Note. — The XD Offset column gives the offset between the Reference and Test exposures, measured as discussed in Section 3.3.

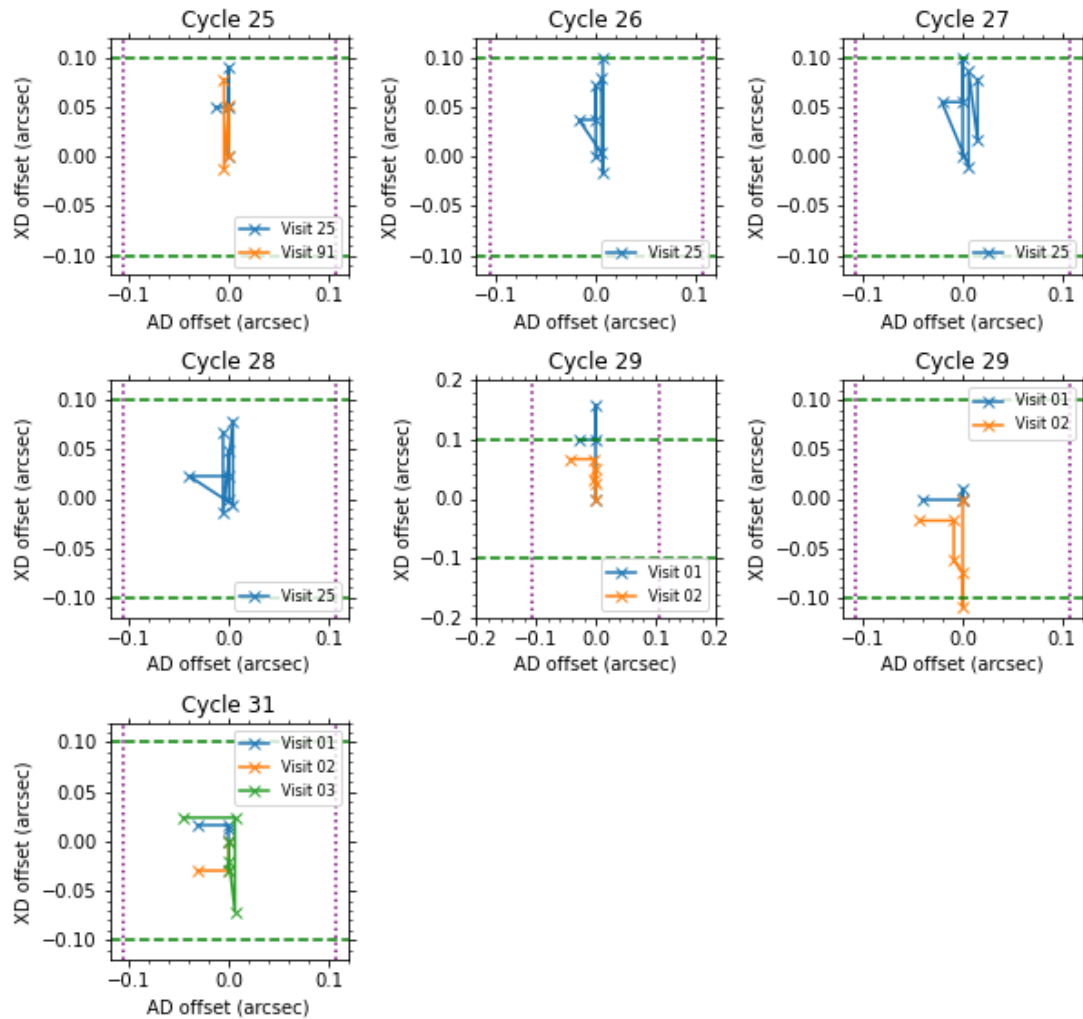


**Figure 4.** For each cycle a separate panel shows the cumulative offset throughout each visit that was part of the FUV TA program. The centered position returned by the initial NUV ACQ/IMAGE is taken to be the (0,0) reference position. Vertical lines linking points indicate the slew in the XD direction resulting from an ACQ/PEAKXD. Horizontal lines linking points indicate the slew in the AD direction resulting from an ACQ/PEAKD. Diagonal lines linking points indicate the slew in both AD and XD directions resulting from an NUV ACQ/IMAGE. The green horizontal dashed lines mark the centering goal of  $\pm 0.1''$  in the XD direction, while the  $\pm 0.3''$  requirement is outside of the plotted regions. Purple vertical dotted lines mark the  $\sim 0.107''$  requirement of the G130M and G160M modes in the AD direction. All FUV TA modes tested center the target to within requirements, and nearly all to within the XD  $1\sigma$  goal.

## References

Bohlin, R. C., Hubeny, I., & Rauch, T. 2024, *AJ*, 160, 21, *New Grids of Pure-hydrogen White Dwarf NLTE Model Atmospheres and the HST/STIS Flux Calibration*.

Dieterich, S., et al. 2024, COS ISR 2024-xx, *The Enabling and Verification of COS FUV Target Acquisition at Lifetime Position 5*.

Hirschauer, A. S. et al. 2023, *Cosmic Origins Spectrograph Instrument Handbook*, Version 16.0 (Baltimore: STScI)

Keyes, C. D., & Penton, S. V. 2010, COS ISR 2010-14, *COS Target Acquisition Guidelines, Recommendations, and Interpretation*.

Penton, S. V., & Keyes, C. D. 2010, COS TIR 2010-03, *On-Orbit Target Acquisitions with HST+COS*.

Penton, S. V., & Sahnou, D. 2023, COS ISR 2023-01, *Cycle 20-24 HST+COS Target Acquisition Monitoring*.

Proffitt, C. R., et al. 2015, COS ISR 2015-03, *Changes to the COS Extraction Algorithm for Lifetime Position 3*.

Rowlands, K., et al. 2024 COS ISR 2024-08, *Simulating the 600 s flash for SPLIT-wavecals at LP6*.

Soderblom, D., et al. 2022, *COS Data Handbook*, Version 5.1, (Baltimore: STScI).

## **Appendix A**

The tables here provide details about the exposure sequences for the cycle 25–31 FUV TA monitoring programs.

**Table A1.** Summary of cycle 25 Observations (15386).

LINENUM	DETECTOR	LP	OPT_ELEM	CENWAVE	(AD, XD) offset (arcsec)	ROOTNAME	Description
G130M test at LP4							
25.001	NUV	1	MIRRORB	...	(0.0, 0.0)	ldqq25g3q	ACQ/IMAGE
25.002	NUV	1	MIRRORB	...	(0.0, 0.0)	ldqq25gbq	EXTERNAL/SCI
25.003	FUV	4	G130M	1291	(0.0, 0.0)	ldqq25gdq	EXTERNAL/SCI
25.004	FUV	4	G130M	1291	(0.0, 1.3)	ldqq25gfq	EXTERNAL/SCI
25.005	FUV	4	G130M	1291	(0.0, -1.3)	ldqq25ghq	EXTERNAL/SCI
25.006	FUV	4	G130M	1291	(0.0, 0.0)	ldqq25gjg	ACQ/PEAKXD
25.007	FUV	4	G130M	1291	(0.0, 0.0)	ldqq25glq	EXTERNAL/SCI
25.008	FUV	4	G130M	1291	(0.0, 1.8)	ldqq25goq	EXTERNAL/SCI
25.009	FUV	4	G130M	1291	(0.0, 0.9)	ldqq25gsq	EXTERNAL/SCI
25.010	FUV	4	G130M	1291	(0.0, -0.9)	ldqq25guq	EXTERNAL/SCI
25.011	FUV	4	G130M	1291	(0.0, -1.8)	ldqq25gwq	EXTERNAL/SCI
25.012	FUV	4	G130M	1291	(0.0, 0.0)	ldqq25hlq	ACQ/PEAKXD
25.013	FUV	4	G130M	1291	(0.0, 0.0)	ldqq25h3q	EXTERNAL/SCI
25.014	FUV	4	G130M	1291	(0.0, 0.0)	ldqq25h6q	ACQ/PEAKD
25.015	FUV	4	G130M	1291	(0.0, 0.0)	ldqq25h8q	EXTERNAL/SCI
Exposures 25.016 through 25.029 failed Exposures 90.001 through 90.014 failed							
G140L test at LP4							
91.001	NUV	1	MIRRORB	...	(0.0, 0.0)	ldqq91v1q	ACQ/IMAGE
91.002	NUV	1	MIRRORB	...	(0.0, 0.0)	ldqq91vnq	EXTERNAL/SCI
91.003	FUV	4	G140L	1280	(0.0, 0.0)	ldqq91vpq	EXTERNAL/SCI
91.004	FUV	4	G140L	1280	(0.0, 1.3)	ldqq91vsq	EXTERNAL/SCI
91.005	FUV	4	G140L	1280	(0.0, -1.3)	ldqq91vuq	EXTERNAL/SCI
91.006	FUV	4	G140L	1280	(0.0, 0.0)	ldqq91vwq	ACQ/PEAKXD
91.007	FUV	4	G140L	1280	(0.0, 0.0)	ldqq91vyq	EXTERNAL/SCI
G160M test at LP4							
91.008	NUV	1	MIRRORB	...	(0.0, 0.0)	ldqq91w0q	ACQ/IMAGE
91.009	NUV	1	MIRRORB	...	(0.0, 0.0)	ldqq91w2q	EXTERNAL/SCI
91.010	FUV	4	G160M	1600	(0.0, 0.0)	ldqq91w4q	EXTERNAL/SCI
91.011	FUV	4	G160M	1600	(0.0, 1.3)	ldqq91w6q	EXTERNAL/SCI
91.012	FUV	4	G160M	1600	(0.0, -1.3)	ldqq91w8q	EXTERNAL/SCI
91.013	FUV	4	G160M	1600	(0.0, 0.0)	ldqq91waq	ACQ/PEAKXD
91.014	FUV	4	G160M	1600	(0.0, 0.0)	ldqq91wcq	EXTERNAL/SCI

Note. — Along-dispersion (AD) and cross-dispersion (XD) offsets are stored in the keywords POSTARG1 and POSTARG2, respectively. The failed exposures in visits 25 and 90 were successfully executed in visit 91.

**Table A2.** Summary of cycle 26 Observations (15537).

LINENUM	DETECTOR	LP	OPT_ELEM	CENWAVE	(AD, XD) offset (arcsec)	ROOTNAME	Description
G130M test at LP4							
25.001	NUV	1	MIRRORB	...	(0.0, 0.0)	ldvq25cpq	ACQ/IMAGE
25.002	NUV	1	MIRRORB	...	(0.0, 0.0)	ldvq25cwq	EXTERNAL/SCI
25.003	FUV	4	G130M	1291	(0.0, 0.0)	ldvq25cyq	EXTERNAL/SCI
25.004	FUV	4	G130M	1291	(0.0, 1.3)	ldvq25d0q	EXTERNAL/SCI
25.005	FUV	4	G130M	1291	(0.0, -1.3)	ldvq25d2q	EXTERNAL/SCI
25.006	FUV	4	G130M	1291	(0.0, 0.0)	ldvq25d4q	ACQ/PEAKXD
25.007	FUV	4	G130M	1291	(0.0, 0.0)	ldvq25d6q	EXTERNAL/SCI
25.008	FUV	4	G130M	1291	(0.0, 1.8)	ldvq25d8q	EXTERNAL/SCI
25.009	FUV	4	G130M	1291	(0.0, 0.9)	ldvq25dbq	EXTERNAL/SCI
25.010	FUV	4	G130M	1291	(0.0, -0.9)	ldvq25ddq	EXTERNAL/SCI
25.011	FUV	4	G130M	1291	(0.0, -1.8)	ldvq25dfq	EXTERNAL/SCI
25.012	FUV	4	G130M	1291	(0.0, 0.0)	ldvq25dkq	ACQ/PEAKXD
25.013	FUV	4	G130M	1291	(0.0, 0.0)	ldvq25dmq	EXTERNAL/SCI
25.014	FUV	4	G130M	1291	(0.0, 0.0)	ldvq25doq	ACQ/PEAKD
25.015	FUV	4	G130M	1291	(0.0, 0.0)	ldvq25dqq	EXTERNAL/SCI
G140L test at LP4							
25.016	NUV	1	MIRRORB	...	(0.0, 0.0)	ldvq25dtq	ACQ/IMAGE
25.017	NUV	1	MIRRORB	...	(0.0, 0.0)	ldvq25dvq	EXTERNAL/SCI
25.018	FUV	4	G140L	1280	(0.0, 0.0)	ldvq25dxq	EXTERNAL/SCI
25.019	FUV	4	G140L	1280	(0.0, 1.3)	ldvq25dzq	EXTERNAL/SCI
25.020	FUV	4	G140L	1280	(0.0, -1.3)	ldvq25e1q	EXTERNAL/SCI
25.021	FUV	4	G140L	1280	(0.0, 0.0)	ldvq25e3q	ACQ/PEAKXD
25.022	FUV	4	G140L	1280	(0.0, 0.0)	ldvq25e5q	EXTERNAL/SCI
G160M test at LP4							
25.023	NUV	1	MIRRORB	...	(0.0, 0.0)	ldvq25e7q	ACQ/IMAGE
25.024	NUV	1	MIRRORB	...	(0.0, 0.0)	ldvq25e9q	EXTERNAL/SCI
25.025	FUV	4	G160M	1600	(0.0, 0.0)	ldvq25ebq	EXTERNAL/SCI
25.026	FUV	4	G160M	1600	(0.0, 1.3)	ldvq25edq	EXTERNAL/SCI
25.027	FUV	4	G160M	1600	(0.0, -1.3)	ldvq25efq	EXTERNAL/SCI
25.028	FUV	4	G160M	1600	(0.0, 0.0)	ldvq25ehq	ACQ/PEAKXD
25.029	FUV	4	G160M	1600	(0.0, 0.0)	ldvq25f6q	EXTERNAL/SCI

**Table A3.** Summary of cycle 27 Observations (15775).

LINENUM	DETECTOR	LP	OPT_ELEM	CENWAVE	(AD, XD) offset (arcsec)	ROOTNAME	Description
G130M test at LP4							
25.001	NUV	1	MIRRORB	...	(0.0, 0.0)	1e5e25k5q	ACQ/IMAGE
25.002	NUV	1	MIRRORB	...	(0.0, 0.0)	1e5e25k7q	EXTERNAL/SCI
25.003	FUV	4	G130M	1291	(0.0, 0.0)	1e5e25k9q	EXTERNAL/SCI
25.004	FUV	4	G130M	1291	(0.0, 1.3)	1e5e25kbq	EXTERNAL/SCI
25.005	FUV	4	G130M	1291	(0.0, -1.3)	1e5e25kdq	EXTERNAL/SCI
25.006	FUV	4	G130M	1291	(0.0, 0.0)	1e5e25kfq	ACQ/PEAKXD
25.007	FUV	4	G130M	1291	(0.0, 0.0)	1e5e25khq	EXTERNAL/SCI
25.008	FUV	4	G130M	1291	(0.0, 1.8)	1e5e25kjq	EXTERNAL/SCI
25.009	FUV	4	G130M	1291	(0.0, 0.9)	1e5e25klq	EXTERNAL/SCI
25.010	FUV	4	G130M	1291	(0.0, -0.9)	1e5e25knq	EXTERNAL/SCI
25.011	FUV	4	G130M	1291	(0.0, -1.8)	1e5e25kpq	EXTERNAL/SCI
25.012	FUV	4	G130M	1291	(0.0, 0.0)	1e5e25krq	ACQ/PEAKXD
25.013	FUV	4	G130M	1291	(0.0, 0.0)	1e5e25ktq	EXTERNAL/SCI
25.014	FUV	4	G130M	1291	(0.0, 0.0)	1e5e25kvq	ACQ/PEAKD
25.015	FUV	4	G130M	1291	(0.0, 0.0)	1e5e25kxq	EXTERNAL/SCI
G140L test at LP4							
25.016	NUV	1	MIRRORB	...	(0.0, 0.0)	1e5e25kzq	ACQ/IMAGE
25.017	NUV	1	MIRRORB	...	(0.0, 0.0)	1e5e25l1q	EXTERNAL/SCI
25.018	FUV	4	G140L	1280	(0.0, 0.0)	1e5e25l3q	EXTERNAL/SCI
25.019	FUV	4	G140L	1280	(0.0, 1.3)	1e5e25l5q	EXTERNAL/SCI
25.020	FUV	4	G140L	1280	(0.0, -1.3)	1e5e25l7q	EXTERNAL/SCI
25.021	FUV	4	G140L	1280	(0.0, 0.0)	1e5e25l9q	ACQ/PEAKXD
25.022	FUV	4	G140L	1280	(0.0, 0.0)	1e5e25lbq	EXTERNAL/SCI
G160M test at LP4							
25.023	NUV	1	MIRRORB	...	(0.0, 0.0)	1e5e25ldq	ACQ/IMAGE
25.024	NUV	1	MIRRORB	...	(0.0, 0.0)	1e5e25lfq	EXTERNAL/SCI
25.025	FUV	4	G160M	1600	(0.0, 0.0)	1e5e25lhq	EXTERNAL/SCI
25.026	FUV	4	G160M	1600	(0.0, 1.3)	1e5e25ljq	EXTERNAL/SCI
25.027	FUV	4	G160M	1600	(0.0, -1.3)	1e5e25llq	EXTERNAL/SCI
25.028	FUV	4	G160M	1600	(0.0, 0.0)	1e5e25lnq	ACQ/PEAKXD
25.029	FUV	4	G160M	1600	(0.0, 0.0)	1e5e25lpq	EXTERNAL/SCI

**Table A4.** Summary of cycle 28 Observations (16326).

LINENUM	DETECTOR	LP	OPT_ELEM	CENWAVE	(AD, XD) offset (arcsec)	ROOTNAME	Description
G130M test at LP4							
25.001	NUV	1	MIRRORB	...	(0.0, 0.0)	1ef925waq	ACQ/IMAGE
25.002	NUV	1	MIRRORB	...	(0.0, 0.0)	1ef925wcq	EXTERNAL/SCI
25.003	FUV	4	G130M	1291	(0.0, 0.0)	1ef925weq	EXTERNAL/SCI
25.004	FUV	4	G130M	1291	(0.0, 1.3)	1ef925wgq	EXTERNAL/SCI
25.005	FUV	4	G130M	1291	(0.0, -1.3)	1ef925wiq	EXTERNAL/SCI
25.006	FUV	4	G130M	1291	(0.0, 0.0)	1ef925wkq	ACQ/PEAKXD
25.007	FUV	4	G130M	1291	(0.0, 0.0)	1ef925wmq	EXTERNAL/SCI
25.008	FUV	4	G130M	1291	(0.0, 1.8)	1ef925woq	EXTERNAL/SCI
25.009	FUV	4	G130M	1291	(0.0, 0.9)	1ef925wqg	EXTERNAL/SCI
25.010	FUV	4	G130M	1291	(0.0, -0.9)	1ef925wsq	EXTERNAL/SCI
25.011	FUV	4	G130M	1291	(0.0, -1.8)	1ef925wuq	EXTERNAL/SCI
25.012	FUV	4	G130M	1291	(0.0, 0.0)	1ef925wwq	ACQ/PEAKXD
25.013	FUV	4	G130M	1291	(0.0, 0.0)	1ef925wyq	EXTERNAL/SCI
25.014	FUV	4	G130M	1291	(0.0, 0.0)	1ef925x0q	ACQ/PEAKD
25.015	FUV	4	G130M	1291	(0.0, 0.0)	1ef925x2q	EXTERNAL/SCI
G140L test at LP4							
25.016	NUV	1	MIRRORB	...	(0.0, 0.0)	1ef925x4q	ACQ/IMAGE
25.017	NUV	1	MIRRORB	...	(0.0, 0.0)	1ef925x6q	EXTERNAL/SCI
25.018	FUV	4	G140L	1280	(0.0, 0.0)	1ef925x8q	EXTERNAL/SCI
25.019	FUV	4	G140L	1280	(0.0, 1.3)	1ef925xaq	EXTERNAL/SCI
25.020	FUV	4	G140L	1280	(0.0, -1.3)	1ef925xcq	EXTERNAL/SCI
25.021	FUV	4	G140L	1280	(0.0, 0.0)	1ef925xeq	ACQ/PEAKXD
25.022	FUV	4	G140L	1280	(0.0, 0.0)	1ef925xgq	EXTERNAL/SCI
G160M test at LP4							
25.023	NUV	1	MIRRORB	...	(0.0, 0.0)	1ef925xiq	ACQ/IMAGE
25.024	NUV	1	MIRRORB	...	(0.0, 0.0)	1ef925xkq	EXTERNAL/SCI
25.025	FUV	4	G160M	1600	(0.0, 0.0)	1ef925xmq	EXTERNAL/SCI
25.026	FUV	4	G160M	1600	(0.0, 1.3)	1ef925xoq	EXTERNAL/SCI
25.027	FUV	4	G160M	1600	(0.0, -1.3)	1ef925xqg	EXTERNAL/SCI
25.028	FUV	4	G160M	1600	(0.0, 0.0)	1ef925xsq	ACQ/PEAKXD
25.029	FUV	4	G160M	1600	(0.0, 0.0)	1ef925xuq	EXTERNAL/SCI

**Table A5.** Summary of cycle 29 Observations (16831).

LINENUM	DETECTOR	LP	OPT_ELEM	CENWAVE	(AD, XD) offset (arcsec)	ROOTNAME	Description
G130M test at LP5							
01.001	NUV	1	MIRRORB	...	(0.0, 0.0)	1er201akq	ACQ/IMAGE
01.002	NUV	1	MIRRORB	...	(0.0, 0.0)	1er201amq	EXTERNAL/SCI
01.003	FUV	5	G130M	1291	(0.0, 0.0)	1er201apq	EXTERNAL/SCI
01.004	FUV	5	G130M	1291	(0.0, 1.3)	1er201arq	EXTERNAL/SCI
01.005	FUV	5	G130M	1291	(0.0, -1.3)	1er201atq	EXTERNAL/SCI
01.006	FUV	5	G130M	1291	(0.0, 0.0)	1er201avq	ACQ/PEAKXD
01.007	FUV	5	G130M	1291	(0.0, 0.0)	1er201axq	EXTERNAL/SCI
01.008	FUV	5	G130M	1291	(0.0, 1.8)	1er201azq	EXTERNAL/SCI
01.009	FUV	5	G130M	1291	(0.0, 0.9)	1er201b1q	EXTERNAL/SCI
01.010	FUV	5	G130M	1291	(0.0, -0.9)	1er201b3q	EXTERNAL/SCI
01.011	FUV	5	G130M	1291	(0.0, -1.8)	1er201b5q	EXTERNAL/SCI
01.012	FUV	5	G130M	1291	(0.0, 0.0)	1er201b7q	ACQ/PEAKXD
01.013	FUV	5	G130M	1291	(0.0, 0.0)	1er201b9q	EXTERNAL/SCI
01.014	FUV	5	G130M	1291	(0.0, 0.0)	1er201bbq	ACQ/PEAKD
01.015	FUV	5	G130M	1291	(0.0, 0.0)	1er201c0q	EXTERNAL/SCI
G140L test at LP4							
02.001	NUV	1	MIRRORB	...	(0.0, 0.0)	1er202n6q	ACQ/IMAGE
02.002	NUV	1	MIRRORB	...	(0.0, 0.0)	1er202n8q	EXTERNAL/SCI
02.003 <sup>a</sup>	FUV	3	G140L	1280	(0.0, 0.0)	1er202naq	EXTERNAL/SCI
02.004 <sup>a</sup>	FUV	3	G140L	1280	(0.0, 1.3)	1er202ncq	EXTERNAL/SCI
02.005 <sup>a</sup>	FUV	3	G140L	1280	(0.0, -1.3)	1er202neq	EXTERNAL/SCI
02.006	FUV	4	G140L	1280	(0.0, 0.0)	1er202ngq	ACQ/PEAKXD
02.007 <sup>a</sup>	FUV	3	G140L	1280	(0.0, 0.0)	1er202niq	EXTERNAL/SCI
02.008 <sup>a</sup>	FUV	3	G140L	1280	(0.0, 1.8)	1er202nkq	EXTERNAL/SCI
02.009 <sup>a</sup>	FUV	3	G140L	1280	(0.0, 0.9)	1er202nmq	EXTERNAL/SCI
02.010 <sup>a</sup>	FUV	3	G140L	1280	(0.0, -0.9)	1er202noq	EXTERNAL/SCI
02.011 <sup>a</sup>	FUV	3	G140L	1280	(0.0, -1.8)	1er202nqq	EXTERNAL/SCI
02.012	FUV	4	G140L	1280	(0.0, 0.0)	1er202nsq	ACQ/PEAKXD
02.013 <sup>a</sup>	FUV	3	G140L	1280	(0.0, 0.0)	1er202nuq	EXTERNAL/SCI
G160M test at LP4							
02.014	NUV	1	MIRRORB	...	(0.0, 0.0)	1er202nwq	ACQ/IMAGE
02.015	NUV	1	MIRRORB	...	(0.0, 0.0)	1er202nyq	EXTERNAL/SCI
02.016	FUV	4	G160M	1600	(0.0, 0.0)	1er202o0q	EXTERNAL/SCI
02.017	FUV	4	G160M	1600	(0.0, 1.3)	1er202o2q	EXTERNAL/SCI
02.018	FUV	4	G160M	1600	(0.0, -1.3)	1er202o4q	EXTERNAL/SCI
02.019	FUV	4	G160M	1600	(0.0, 0.0)	1er202o6q	ACQ/PEAKXD
02.020	FUV	4	G160M	1600	(0.0, 0.0)	1er202o8q	EXTERNAL/SCI
02.021	FUV	4	G160M	1600	(0.0, 0.0)	1er202o9q	ACQ/PEAKD
02.022	FUV	4	G160M	1600	(0.0, 0.0)	1er202ocq	EXTERNAL/SCI

<sup>a</sup>At the time of execution, the default location for G140L science observations was LP3, while the default location for G140L target acquisition was LP4. Due to a missing Optional Parameter in APT, the test observations were executed at the wrong LP.

**Table A6.** Summary of cycle 30 Observations (16942).

LINENUM	DETECTOR	LP	OPT_ELEM	CENWAVE	(AD, XD) offset (arcsec)	ROOTNAME	Description
G130M test at LP5							
01.001	NUV	1	MIRRORB	...	(0.0, 0.0)	lewz01i4q	ACQ/IMAGE
01.002	NUV	1	MIRRORB	...	(0.0, 0.0)	lewz01i6q	EXTERNAL/SCI
01.003	FUV	5	G130M	1291	(0.0, 0.0)	lewz01i8q	EXTERNAL/SCI
01.004	FUV	5	G130M	1291	(0.0, 1.3)	lewz01iaq	EXTERNAL/SCI
01.005	FUV	5	G130M	1291	(0.0, -1.3)	lewz01icq	EXTERNAL/SCI
01.006	FUV	5	G130M	1291	(0.0, 0.0)	lewz01ieq	ACQ/PEAKXD
01.007	FUV	5	G130M	1291	(0.0, 0.0)	lewz01iqq	EXTERNAL/SCI
01.008	FUV	5	G130M	1291	(0.0, 1.8)	lewz01iiq	EXTERNAL/SCI
01.009	FUV	5	G130M	1291	(0.0, 0.9)	lewz01ikq	EXTERNAL/SCI
01.010	FUV	5	G130M	1291	(0.0, -0.9)	lewz01imq	EXTERNAL/SCI
01.011	FUV	5	G130M	1291	(0.0, -1.8)	lewz01ioq	EXTERNAL/SCI
01.012	FUV	5	G130M	1291	(0.0, 0.0)	lewz01iqq	ACQ/PEAKXD
01.013	FUV	5	G130M	1291	(0.0, 0.0)	lewz01isq	EXTERNAL/SCI
01.014	FUV	5	G130M	1291	(0.0, 0.0)	lewz01iuq	ACQ/PEAKD
01.015	FUV	5	G130M	1291	(0.0, 0.0)	lewz01izq	EXTERNAL/SCI
G140L test at LP4							
02.001	NUV	1	MIRRORB	...	(0.0, 0.0)	lewz02pdq	ACQ/IMAGE
02.002	NUV	1	MIRRORB	...	(0.0, 0.0)	lewz02pfq	EXTERNAL/SCI
02.003	FUV	3	G140L	1280	(0.0, 0.0)	lewz02phq	EXTERNAL/SCI
02.004	FUV	4	G140L	1280	(0.0, 0.0)	lewz02pjg	EXTERNAL/SCI
02.005	FUV	4	G140L	1280	(0.0, 1.3)	lewz02plq	EXTERNAL/SCI
02.006	FUV	4	G140L	1280	(0.0, -1.3)	lewz02pnq	EXTERNAL/SCI
02.007	FUV	4	G140L	1280	(0.0, 0.0)	lewz02ppq	ACQ/PEAKXD
02.008	FUV	3	G140L	1280	(0.0, 0.0)	lewz02prq	EXTERNAL/SCI
02.009	FUV	4	G140L	1280	(0.0, 0.0)	lewz02ptq	EXTERNAL/SCI
02.010	FUV	4	G140L	1280	(0.0, 1.8)	lewz02pvq	EXTERNAL/SCI
02.011	FUV	4	G140L	1280	(0.0, 0.9)	lewz02pxq	EXTERNAL/SCI
02.012	FUV	4	G140L	1280	(0.0, -0.9)	lewz02pzq	EXTERNAL/SCI
02.013	FUV	4	G140L	1280	(0.0, -1.8)	lewz02q1q	EXTERNAL/SCI
02.014	FUV	4	G140L	1280	(0.0, 0.0)	lewz02q3q	ACQ/PEAKXD
02.015	FUV	3	G140L	1280	(0.0, 0.0)	lewz02q5q	EXTERNAL/SCI
G160M test at LP4							
02.016	NUV	1	MIRRORB	...	(0.0, 0.0)	lewz02q7q	ACQ/IMAGE
02.017	NUV	1	MIRRORB	...	(0.0, 0.0)	lewz02q9q	EXTERNAL/SCI
02.018	FUV	4	G160M	1600	(0.0, 0.0)	lewz02qbq	EXTERNAL/SCI
02.019	FUV	4	G160M	1600	(0.0, 1.3)	lewz02qdq	EXTERNAL/SCI
02.020	FUV	4	G160M	1600	(0.0, -1.3)	lewz02qgq	EXTERNAL/SCI
02.021	FUV	4	G160M	1600	(0.0, 0.0)	lewz02qiq	ACQ/PEAKXD
02.022	FUV	4	G160M	1600	(0.0, 0.0)	lewz02qkq	EXTERNAL/SCI
02.023	FUV	4	G160M	1600	(0.0, 0.0)	lewz02qmq	ACQ/PEAKD
02.024	FUV	4	G160M	1600	(0.0, 0.0)	lewz02rbq	EXTERNAL/SCI

Note. — Program 16942 contains another visit (03) for LP6 TA enabling purposes that will be discussed in a future ISR.

**Table A7.** Summary of cycle 31 Observations (17582).

LINENUM	DETECTOR	LP	OPT.ELEM	CENWAVE	(AD, XD) offset (arcsec)	ROOTNAME	Description
G130M test at LP5							
01.001	NUV	1	MIRRORB	...	(0.0, 0.0)	lfaw01dpq	ACQ/IMAGE
01.002	NUV	1	MIRRORB	...	(0.0, 0.0)	lfaw01drq	EXTERNAL/SCI
01.003	FUV	5	G130M	1291	(0.0, 0.0)	lfaw01dtq	EXTERNAL/SCI
01.004	FUV	5	G130M	1291	(0.0, 1.3)	lfaw01dvq	EXTERNAL/SCI
01.005	FUV	5	G130M	1291	(0.0, -1.3)	lfaw01dxq	EXTERNAL/SCI
01.006	FUV	5	G130M	1291	(0.0, 0.0)	lfaw01dzq	ACQ/PEAKXD
01.007	FUV	5	G130M	1291	(0.0, 0.0)	lfaw01e1q	EXTERNAL/SCI
01.008	FUV	5	G130M	1291	(0.0, 1.8)	lfaw01e3q	EXTERNAL/SCI
01.009	FUV	5	G130M	1291	(0.0, 0.9)	lfaw01e5q	EXTERNAL/SCI
01.010	FUV	5	G130M	1291	(0.0, -0.9)	lfaw01e7q	EXTERNAL/SCI
01.011	FUV	5	G130M	1291	(0.0, -1.8)	lfaw01e9q	EXTERNAL/SCI
01.012	FUV	5	G130M	1291	(0.0, 0.0)	lfaw01ebq	ACQ/PEAKXD
01.013	FUV	5	G130M	1291	(0.0, 0.0)	lfaw01edq	EXTERNAL/SCI
01.014	FUV	5	G130M	1291	(0.0, 0.0)	lfaw01efq	ACQ/PEAKD
01.015	FUV	5	G130M	1291	(0.0, 0.0)	lfaw01ehq	EXTERNAL/SCI
G160M test at LP4							
02.001	NUV	1	MIRRORB	...	(0.0, 0.0)	lfaw02a8q	ACQ/IMAGE
02.002	NUV	1	MIRRORB	...	(0.0, 0.0)	lfaw02abq	EXTERNAL/SCI
02.003	FUV	4	G160M	1600	(0.0, 0.0)	lfaw02aeq	EXTERNAL/SCI
02.004	FUV	4	G160M	1600	(0.0, 1.3)	lfaw02agq	EXTERNAL/SCI
02.005	FUV	4	G160M	1600	(0.0, -1.3)	lfaw02alq	EXTERNAL/SCI
02.006	FUV	4	G160M	1600	(0.0, 0.0)	lfaw02anq	ACQ/PEAKXD
02.007	FUV	4	G160M	1600	(0.0, 0.0)	lfaw02apq	EXTERNAL/SCI
02.008	FUV	4	G160M	1600	(0.0, 0.0)	lfaw02arq	ACQ/PEAKD
02.009	FUV	4	G160M	1600	(0.0, 0.0)	lfaw02atq	EXTERNAL/SCI
G140L test at LP4							
03.001	NUV	1	MIRRORB	...	(0.0, 0.0)	lfaw03feq	ACQ/IMAGE
03.002	NUV	1	MIRRORB	...	(0.0, 0.0)	lfaw03fgq	EXTERNAL/SCI
03.003	FUV	4	G140L	1280	(0.0, 0.0)	lfaw03fiq	EXTERNAL/SCI
03.004	FUV	4	G140L	1280	(0.0, 1.3)	lfaw03fkq	EXTERNAL/SCI
03.005	FUV	4	G140L	1280	(0.0, -1.3)	lfaw03fmq	EXTERNAL/SCI
03.006	FUV	4	G140L	1280	(0.0, 0.0)	lfaw03foq	ACQ/PEAKXD
03.007	FUV	4	G140L	1280	(0.0, 0.0)	lfaw03fqq	EXTERNAL/SCI
03.008	FUV	4	G140L	1280	(0.0, 1.8)	lfaw03ftq	EXTERNAL/SCI
03.009	FUV	4	G140L	1280	(0.0, 0.9)	lfaw03fvq	EXTERNAL/SCI
03.010	FUV	4	G140L	1280	(0.0, -0.9)	lfaw03fxq	EXTERNAL/SCI
03.011	FUV	4	G140L	1280	(0.0, -1.8)	lfaw03fzq	EXTERNAL/SCI
03.012	FUV	4	G140L	1280	(0.0, 0.0)	lfaw03glq	ACQ/PEAKXD
03.013	FUV	4	G140L	1280	(0.0, 0.0)	lfaw03g3q	EXTERNAL/SCI
G160M test at LP6							
03.014	NUV	1	MIRRORB	...	(0.0, 0.0)	lfaw03gcq	ACQ/IMAGE
03.015	NUV	1	MIRRORB	...	(0.0, 0.0)	lfaw03geq	EXTERNAL/SCI
03.016	FUV	6	G160M	1600	(0.0, 0.0)	lfaw03ggq	EXTERNAL/SCI
03.017	FUV	6	G160M	1600	(0.0, 1.3)	lfaw03giq	EXTERNAL/SCI
03.018	FUV	6	G160M	1600	(0.0, -1.3)	lfaw03gkq	EXTERNAL/SCI
03.019	FUV	6	G160M	1600	(0.0, 0.0)	lfaw03gmq	ACQ/PEAKXD
03.020	FUV	6	G160M	1600	(0.0, 0.0)	lfaw03goq	EXTERNAL/SCI
03.021	FUV	6	G160M	1600	(0.0, 0.0)	lfaw03gqq	ACQ/PEAKD
03.022	FUV	6	G160M	1600	(0.0, 0.0)	lfaw03gsq	EXTERNAL/SCI